A New Procedure for the Optimization of a Dielectric Elastomer Actuator

Rocco Vertechy

PERCRO Laboratory,
Scuola Superiore Sant'Anna, Italy
E-mail: r.vertechy@sssup.it

Giovanni Berselli, Vincenzo Parenti Castelli, and Gabriele Vassura

Department of Mechanical and Aeronautical Engineering,
University of Bologna, Italy
E-mail: {giovanni.berselli, vincenzo.parenti, gabriele.vassura}@unibo.it

Abstract A novel mathematical procedure is proposed, which makes it possible to optimize lozenge-shaped dielectric-elastomer-based linear actuators for known materials and desired force/stroke requirements. Simulation results are provided which both demonstrate the efficacy of the novel procedure with respect to traditional design approaches and show that simpler, cheaper, lighter and better-behaved lozenge-shaped actuators can be conceived which do not require any integration of compliant frame elements.

1. Introduction

Dielectric Elastomers (DE) are deformable dielectrics which can experience isochoric finite deformations in response to applied large electric fields [1]. Thanks to the strong electro-mechanical coupling, DE intrinsically offer great potentialities for conceiving novel solid-state mechatronic devices, such as sensors and actuators, which are more integrated, lightweight, economic, silent, resilient and disposable than equivalent systems based on traditional technologies [2].

For actuation usage, DE are usually shaped in thin films coated with compliant electrodes on both sides and piled one on the other to form an Electro-Active Film (EAF) [1-4]. Activation of the EAF via the placement of differential electric potentials (hereafter also called voltages) between the electrodes can induce film

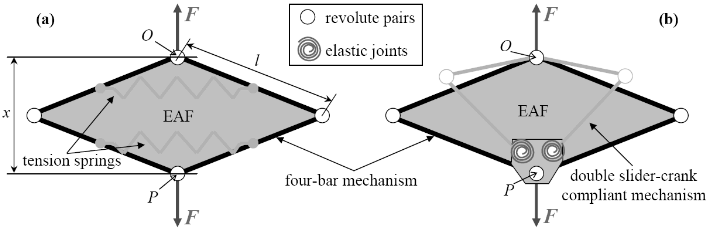

Fig. 1 Lozenge-shaped DE-based linear actuators

area expansions and, thus, point's displacements which can be used to produce useful mechanical work (whenever forces are applied to such points).

Usually, DE-based actuators are obtained by first uniformly pre-stretching the EAF (which is necessary since the film has negligible flexural rigidity) and then by coupling some segment of its boundary to some portion of a flexible supporting frame [3-5]. The major roles of the flexible frame are: 1) to coerce the EAF expansion in preferred directions; 2) to maintain the EAF in a tensioned state so as to prevent buckling effects; and 3) to provide a desired actuator stiffness characteristic (typically a nearly naught stiffness through the whole actuator stroke). Practical examples of DE-based linear actuators are depicted in Figs. 1.a and 1.b. The actuators are based on a lozenge-shaped pre-stretched EAF coupled to elastic frames made by a four-bar mechanism with equal links and either two identical non-linear tension springs (Fig. 1.a, [3]) or a compliant symmetric double slider-crank mechanism with elastic joints on the slider pivots (Fig. 1.b, [5]). As depicted in Fig. 2, in such actuators, activation of the EAF makes it possible to control the relative distance x (hereafter also called "EAF length" or "actuator length") of the centers O and P of two opposing revolute pairs of the four-bar mechanism, which are the points of application of the external forces F.

The actual procedure for designing DE-based actuators consists in first selecting the appropriate EAF topology; second, empirically determining EAF pre-stretches and dimensions; and, finally, mathematically or experimentally designing a flexible polymeric frame which complies with points 1-3 described above. Although valid, this procedure is not rigorous, neither provides optimal actuators.

In this paper a novel procedure is proposed for the optimal design of lozenge-shaped DE-based linear actuators like the one depicted in Fig. 2. The procedure is efficient, based on a mathematical model and makes it possible to improve the

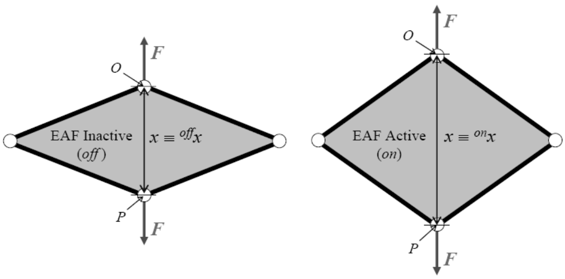

Fig. 2 Inactive (*off*) and active (*on*) lozenge-shaped DE-based linear actuator

actuator force/stroke performance while, at the same time, eliminating the need of supporting frame compliant elements (which simplify the DE-based actuator drastically).

2. General aspects of DE-based actuator design

By definition [1], DE are incompressible, hyper-elastic linear dielectrics whose electrical polarization is fairly independent of material deformation. For such materials, it is well known that EAF activation generates an electric field, $E = V/t$ (V being the activation voltage applied between the EAF electrodes and t is the actual thickness of the DE film amid the EAF electrodes), and an electrically-induced Cauchy stress, $\sigma_{em} = \varepsilon E^2$ (ε being the DE electric permittivity), both acting in the DE film thickness direction. Consequently, the mechanical stress field in a stretched and activated single-layered EAF, which is free to deform in its thickness direction, is given by the following relationships [6]

$$\sigma_1 = \lambda_1 \frac{\partial\Psi}{\partial\lambda_1} - \sigma_{em}, \ \sigma_2 = \lambda_2 \frac{\partial\Psi}{\partial\lambda_2} - \sigma_{em} \text{ and } \sigma_3 = -\sigma_{em} = -\varepsilon \frac{V^2}{\lambda_3^2 t_0^2} \tag{1}$$

where λ_i and σ_i (i = 1, 2, 3) are, respectively, the principal stretches and the Cauchy stresses (the third principal direction coinciding with the film thickness direction), $\Psi = \Psi(\lambda_1, \lambda_2)$ is the incompressible DE strain-energy function [6] and t_0 is the unstretched DE film thickness. For the incompressibility condition $\lambda_3 = 1/\lambda_1\lambda_2$ holds.

By construction, when coupled with a four-bar mechanism having links of equal length, lozenge-shaped EAFs expand uniformly without changing their edge length l and principal stretch/stress directions [4]. Thus, their deformation state is characterized by the following principal stretches

$$\lambda_1 = \lambda_{1,p}\, x/x_p \, , \ \lambda_2 = \lambda_{2,p} \sqrt{\left(4l^2 - x^2\right)/\left(4l^2 - x_p^2\right)} \tag{2}$$

where, referring to Figs. 1 and 2, $\lambda_{1,p}$ and $\lambda_{2,p}$ are the EAF principal pre-stretches in the configuration where $x \equiv x_p$ (x_p can be chosen as desired). Of course, the first and second principal stretch/stress directions are respectively aligned and orthogonal to the line joining the points O and P. The external forces (either force off, ${}^{off}F$, or force on, ${}^{on}F$, depending on the EAF activation state) that must be supplied at O and P, and directed along the line joining these points, to balance the EAF stress field are [4, 8]

$${}^{off}F(x) = \frac{t_0}{2}\left[\partial\Psi/\partial\lambda_1 \sqrt{4l^2 - x_p^2}\Big/\lambda_{2,p} - \partial\Psi/\partial\lambda_2\, x x_p\Big/\sqrt{\lambda_{1,p}^2\left(4l^2 - x^2\right)}\right], \tag{3.1}$$

$$^{on}F\left(x,V\right) = {}^{off}F\left(x\right) + {}^{em}F\left(x,V\right), \tag{3.2}$$

$$^{em}F\left(x,V\right) = -\left[\varepsilon V^{2}\lambda_{1,p}\lambda_{2,p}x\left(2l^{2}-x^{2}\right)\right]\Big/\left[t_{0}x_{p}\sqrt{4l^{2}-x_{p}^{2}}\right], \tag{3.3}$$

which, by convention, are positive if directed according to the arrows depicted in Figs. 1 and 2. Note that $^{em}F(x,V)$, given by Eq. (3,3), is an "electric" force due to EAF activation.

The mathematical Force-Length (FL) curves, $^{off}F(x)$ and $^{on}F(x,V)$, obtained by Eqs. (1-3) for different values of activation voltages (respectively for V = 0V and V = 2.2kV, V = 6.5kV, V = 8.7kV) are plotted in Fig. 3 for a typical lozenge shaped EAF, composed of a single acrylic DE (3M-VHB 4905) and two silver conductive grease electrodes (CircuitWorks-CW7100). The film pre-stretches are $\lambda_{1,p}$ = 2.2 and $\lambda_{2,p}$ = 5 (as recommended in [3, 4]); the film dimensions are t_0 = 1.5 mm, l = 70mm and x_p = 15mm. The mathematical curves are obtained by using a first-order Ogden type [6] strain-energy function Ψ, $\Psi = (\mu / \alpha)\ (\lambda_1^{\alpha} + \lambda_2^{\alpha} + \lambda_1^{-\alpha}\lambda_2^{-\alpha} - 3)$ with parameters μ = 60kPa and α = 1.8, and a DE electric permittivity $\varepsilon = 4.5 \cdot 8.85\text{e}^{-12}$F/m [4]. The figure shows that the EAF curves $^{off}F(x)$ and $^{on}F(x,V)$ are usually nonparallel and nonlinear. This complicates the DE-based actuator design and control. Indeed, a well-behaved actuator should feature linear (typically with zero slope) FL curves and available thrust $T(x)$, $T(x) = [{}^{off}F(x) - {}^{on}F(x,V_{max})]$ (V_{max} being the maximum operating voltage), independent of the actuator length, x.

To face this issue, traditional design procedures propose to couple EAF (of experimentally predefined pre-stretch and geometry) with suitably sized elastic frames made of polymeric materials [3-5]. That is, the actual design procedure for lozenge-shaped DE actuators consists in the following sequential steps: i) empirical determination of film pre-stretches which guarantee the maximal area expansion of the activated EAF [3, 4]; ii) experimental determination of EAF geometrical dimensions which satisfy given actuator force/stroke requirements [3, 4]; iii) mathematical or experimental design of the elastic frame [3-5]. Although valid, this design approach is not rigorous, neither provides optimal actuators. Indeed, elastic frames can only linearize either the $^{off}F(x)$ or $^{on}F(x,V)$ EAF curves. Moreover, by introducing more components, the resulting actuators become bulkier, heavier, more expensive and complex, and are likely to show degraded efficiency, reliability and repeatability.

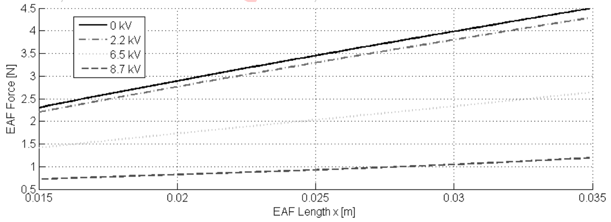

Fig. 3 Force-Length (FL) curves of a typical lozenge-shaped EAF

3. The novel design approach

In this section, a mathematical procedure is described that makes it possible to design well-behaved lozenge-shaped DE-based actuators, which do not need to be coupled with properly dimensioned compliant frames.

Consider the adimensional parameter $\chi = x/l$ which uniquely identifies the lozenge configuration. Differently from the actual design procedure, the proposed approach has the following sequential steps: i) given the desired initial and final actuator lengths, x_i and x_f (thus the ratio $\delta = x_i/x_f$), identify the range of lozenge configurations, $[\delta\chi_f, \chi_f]$ ($\chi_f = x_f/l$ being the final configuration), that minimizes the maximum actuator thrust relative error $\underline{e}_T$, $\underline{e}_T = [\max(T(x))/\min(T(x)) - 1]$ within $x_i \le x \le x_f$; ii) find the lozenge geometry which satisfies the desired actuator lengths, x_f and x_i, and the desired force thrust $\underline{T}$, $\underline{T} = \min[T(x)]$ within $x_i \le x \le x_f$, for a given maximum bearable (limiting) electric field E_l; iii) find the EAF prestretches which, besides preventing film failures (rupture) and buckling, guarantee the desired linear FL curve, ${}^{off}\underline{F}$, of the actuator in its inactive state.

3.1 Mathematical insights on the EAF force

Posing $E_l = E_f = V/t_f$ (t_f being the DE film thickness in the final actuator configuration) and, momentarily, $\chi_p = \chi_f$, equations (3.1) and (3.3) can be rewritten as

$$ {}^{off}F = {}^{off}f\left(\chi, \lambda_{1,p}, \lambda_{2,p}\right) l t_f \chi_f \sqrt{1-\chi_f^2/4}\,, \tag{4.1}$$

$$ {}^{em}F = {}^{em}f\left(\chi\right)\left(l t_f \varepsilon E_l^2\right) \Big/ \left(\chi_f \sqrt{4-\chi_f^2}\right), \tag{4.2}$$

where

$$ {}^{off}f = \left(\partial\Psi/\partial\lambda_1\right)\lambda_1/\chi - \left(\partial\Psi/\partial\lambda_2\right)\lambda_2\chi \big/ \left(4-\chi^2\right) \text{ and } {}^{em}f = \chi\left(\chi^2-2\right) \tag{4.3}$$

which show that the thrust relative error, $(T(x)/\underline{T} - 1)$, depends on χ (and thus on $\delta = x_i/x_f$) only, while the nonlinearity of ${}^{off}F(x)$, and thus of ${}^{on}F(x,V)$, depends on χ, $\lambda_{1,p}$, $\lambda_{2,p}$ and on the DE mechanical properties hidden in the strain-energy function. A plot of the adimensional "electric" force, ${}^{em}f$, is given in Fig. 4 which highlights that the EAF can sustain significant compressive external forces only if $\chi_f \le 2^{0.5}$ and provide a quasi constant thrust $T(x)$ if $\delta\chi_f$ and χ_f are close to 0.8. Therefore, in this paper $\chi_f \le 2^{0.5}$ is considered only. Note that if $\chi_f \le 2^{0.5}$, the maximum electric field E, which acts on the DE for a given electric potential V, is at χ_f (i.e. the actuator configuration for which EAF area and thickness are maximum and minimum respectively), for this reason $E_l = E_f$ has been posed in Eqs. (4).

3.2 The optimization procedure

Following the considerations highlighted in section 3.1, actuator optimization can be conducted according to the following sequential steps:

1) Given the desired initial and final actuator lengths, x_i and x_f (and thus $\delta = x_i/x_f$), then find χ_f that minimizes $\underline{e}_T$, i.e.

$$\chi_f = \sqrt{2/\left(\delta^2 + \delta + 1\right)}\ ; \tag{5}$$

2) Given χ_f and the desired final actuator length x_f solve for the lozenge length $l = x_f/\chi_f$;

3) Given χ_f, l, the DE electrical properties, ε and E_l, and the desired thrust $\underline{T}$ find t_f as

$$t_f = \left[\chi_f \sqrt{4-\chi_f^2}\,\underline{T}\right] \Big/ \left[{}^{em}f\left(\chi_f\right) l \varepsilon E_l^2\right]; \tag{6}$$

4) Given χ_f, l, t_f, the DE mechanical properties and a desired force profile ${}^{off}\underline{F}(x)$, find $\underline{\lambda}_{1,p}$ and $\underline{\lambda}_{2,p}$ that minimize

$$\Im\left(\lambda_{1,p}, \lambda_{2,p}\right) = \int_{x_i}^{x_f} \left[{}^{off}F\left(x, \lambda_{1,p}, \lambda_{2,p}\right) - {}^{off}\underline{F}\left(x\right)\right]^2 dx\,, \tag{7.1}$$

subjected to the following anti-failure criteria

$$\left[\sigma_1\left(x, \underline{\lambda}_{1,p}, \underline{\lambda}_{2,p}\right) > 0\right]\ \&\ \left[\sigma_2\left(x, \underline{\lambda}_{1,p}, \underline{\lambda}_{2,p}\right) > 0\right], \forall x \in \left[x_i, x_f\right], \tag{7.2}$$

$$\Phi\left(\lambda_1\left(x\right), \lambda_2\left(x\right)\right) < 0, \forall x \in \left[x_i, x_f\right], \tag{7.3}$$

where the relations (7.2) are derived from Eq. (1) and guarantee that the EAF will not buckle in the desired actuator range of motion, and Φ is a suitable fracture criterion of the DE [7];

5) Given t_f, $\underline{\lambda}_{1,p}$ and $\underline{\lambda}_{2,p}$ find the unstretched film thickness as $t_0 = t_f\, \underline{\lambda}_{1,p} \underline{\lambda}_{2,p}$.

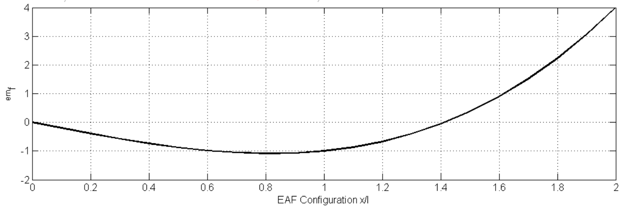

Fig. 4 Adimensional electric force ${}^{em}f$ vs EAF configuration x/l

4. Case study

The procedure presented in Section 3.2 has been used for designing a linear actuator. The actuator position requirements are x_i = 15mm and x_f = 35mm (thus δ = 0.43); the actuator force requirements are a tensile force $^{off}\underline{F}(x)$ = +0.5N, a compressive force $^{on}\underline{F}(x,V_{max})$ = –1N, and thus an available thrust $\underline{T}$ = 1.5N. The DE and electrode materials are the same as those used for the example examined in Fig. 3, that is an acrylic DE (3M-VHB 4905) and silver conductive grease electrodes (CircuitWorks-CW7100) such that $\varepsilon = 4.5\cdot 8.85e^{-12}$F/m, μ = 60kPa and α = 1.8. The Kawabata's criterion [7]

$$\Phi(\lambda_1(x),\lambda_2(x)) = \max_{x\in[x_i,x_f]}[\lambda_1(x),\lambda_2(x)] < 9, \tag{8}$$

is used to check for DE mechanical rupture. To avoid DE electric breakdown, the limiting electric field is set to E_l = 150MV/m.

The resulting actuator geometrical dimensions are χ_f = 1.113, l = 31mm, $\underline{\lambda}_{1,p}$ = 2.12 and $\underline{\lambda}_{2,p}$ = 8.18 (referred to x_p = 15mm), and t_0 = 4mm. For safety reasons, limiting the required electric potential V below 10kV, the resulting EAF is subdivided in two layers each having t_0 = 2mm. Note that, for the given DE material, these design parameters are obtained analytically. The mathematical Force-Length (FL) curves, $^{off}F(x)$ and $^{on}F(x,V)$, of the optimized actuator are plotted in Fig. 5 for different values of activation voltages (respectively for V = 0V and V = 2.2kV, V = 6.5kV, V = 8.7kV). As shown, the EAFs fully satisfy the desired actuator force/stroke requirements. The FL curves are nearly constant independently of the activation voltages. The maximum (at V_{max} = 8.7kV) thrust relative error is $\underline{e}_T$ = 28% (of $\underline{T}$ = 1.5N). Comparison between Figs. 3 and 5 highlights that the optimized EAF performs better than the typical EAF designed according to the conventional design procedure. Indeed, for the latter, the FL curves are non-parallel, with slope depending on the activation voltage, and the maximum (at V_{max} = 8.7kV) thrust relative error is $\underline{e}_T$ = 108% (of $\underline{T}$ = 1.58N). This demonstrates that the empirical condition, $7 \le \underline{\lambda}_{1,p}\cdot\underline{\lambda}_{2,p} \le 11$ that maximizes the free area expansion of EAF, which was suggested in [3, 4] for choosing the film pre-stretches at x_i is not a necessary one for lozenge-shaped DE-based linear actuators.

Note that, while the optimized EAF can simply be coupled to a four-bar mechanism, in order to satisfy the desired $^{off}\underline{F}(x)$ = 0.5N, the typical EAF requires a com-

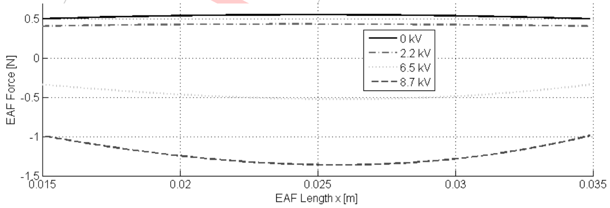

Fig. 5 Force-Length (FL) curves of the optimized lozenge-shaped EAF

pliant frame which, besides bringing design, manufacturing, reliability and efficiency issues, is likely to worsen $\underline{e}_T$. In addition, it can be shown [8] that the optimized EAF has lower lateral encumbrance, requires less DE material for producing the same actuator thrust, and has smaller electric time constant than the typical EAF (i.e. the optimized actuator will have better dynamic response, and will be easier to drive and control than the actuator designed according to the traditional procedure).

5. Conclusions

A novel mathematically based procedure for the optimization of lozenge-shaped dielectric-elastomer-based linear actuators has been presented. The procedure has been applied to a case study. Simulation results showed that traditional design approaches are not rigorous and neither provides actuators with optimal performances, while the novel procedure makes it possible to develop improved actuators having elastic-less frames, maximum force density and reduced electrical activation requirements.

References

[1] Pelrine, R.E., Kornbluh, R.D., and Joseph, J., 1998. “Electrostriction of polymer dielectrics with compliant electrodes as a means of actuation”, *Sensors and Actuators A*, **64**, pp. 77–85.

[2] Bar-Cohen, J., 2001. *Electroactive Polymer (EAP) Actuators as Artificial Muscles: Reality, Potential and Challenges*. Bellingham, WA, SPIE Press.

[3] Vogan, J., 2004. "Development of Dielectric Elastomer Actuators for MRI Devices". *M.S. Thesis*, Department of Mechanical Engineering, Massachusetts Institute of Technology, Cambridge, MA.

[4] Plante, J.S., 2006. "Dielectric elastomer actuators for binary robotics and mechatronics". *Ph.D. Thesis*, Department of Mechanical Engineering, Massachusetts Institute of Technology, Cambridge, MA.

[5] Berselli, G., Vertechy, R., Vassura, G., and Parenti Castelli, V., 2008. "A compound-structure frame for improving the performance of a Dielectric Elastomer Actuator". *Advances in Robot Kinematics: Analysis and Design*, Springer Netherlands, ISBN: 978-1-4020-8599-4, pp. 291-299.

[6] Holzapfel, G.A., 2001. *Nonlinear Solid Mechanics: A Continuum Approach for Engineering*, John Wiley & Sons.

[7] Hamdi, A., Nait Abdelaziz, M., Ait Hocine, N., Heuillet, P., and Benseddiq, N., 2006. “A fracture criterion of rubber-like materials under plane stress conditions”. *Polymer Testing*, **25**(8), pp. 994-1005.

[8] Vertechy, R., Berselli, G., Parenti Castelli, V. and Vassura, G., 2008,. “A New Procedure for the Optimization of a Dielectric Elastomer Actuator”, *Proceedings of II Giornata Ettore Funaioli*, University of Bologna, Bologna, Italy.